

Alternative Brain Connectivity Underscores Age-Related Differences in the Processing of Interactive Biological Motion

 Jon Walbrin,^{1,2}  Jorge Almeida,^{1,2} and  Kami Koldewyn³

¹Proaction Laboratory, Faculty of Psychology and Educational Sciences, University of Coimbra, Coimbra, Portugal 3000-481, ²CINEICC, Faculty of Psychology and Educational Sciences, University of Coimbra, Coimbra, Portugal 3000-481, and ³School of Human and Behavioural Sciences, Bangor University, Bangor, Wales 3000-481

Rapidly recognizing and understanding others' social interactions is an important ability that relies on deciphering multiple sources of information, for example, perceiving body information and inferring others' intentions. Despite recent advances in characterizing the brain basis of this ability in adults, its developmental underpinnings are virtually unknown. Here, we used fMRI to investigate which sources of social information support superior temporal sulcus responses to interactive biological motion (i.e., 2 interacting point-light human figures) at different developmental intervals in human participants (of either sex): Children show supportive functional connectivity with key nodes of the mentalizing network, while adults show stronger reliance on regions associated with body- and dynamic social interaction/biological motion processing. We suggest that adults use efficient action-intention understanding via body and biological motion information, while children show a stronger reliance on hidden mental state inferences as a potential means of learning to better understand others' interactive behavior.

Key words: biological motion; connectivity; development; mentalizing; social interaction; superior temporal sulcus

Significance Statement

Recognizing others' interactive behavior is a critical human skill that depends on different sources of social information (e.g., observable body-action information, inferring others' hidden mental states, etc.). Understanding the brain-basis of this ability and characterizing how it emerges across development are important goals in social neuroscience. Here, we used fMRI to investigate which sources of social information support interactive biological motion processing in children (6–12 years) and adults. These results reveal a striking developmental difference in terms of how wider-brain connectivity shapes functional responses to interactive biological motion that suggests a reliance on distinct neuro-cognitive strategies in service of interaction understanding (i.e., children and adults show a greater reliance on explicit and implicit intentional inference, respectively).

Introduction

Rapidly understanding the contents of others' social interactions is an indispensable ability that is achieved via different levels of appraisal (e.g., extracting perceptual and action-related information

from visible body-based cues, or making inferences about the hidden mental states of interactors) (Quadflieg and Koldewyn, 2017). Recent fMRI work demonstrates that regions within posterior temporal cortex are important for the visual analysis of body-based interactions; for example, extrastriate body area (EBA) and fusiform body area (FBA) (e.g., Downing et al., 2006) are sensitive to the spatial relations between human body dyads that convey or imply interactive behavior (Quadflieg et al., 2015; Walbrin and Koldewyn, 2019; Abassi and Papeo, 2020; Landsiedel et al., 2022).

Similarly, superior temporal sulcus (STS), especially posterior STS (PSTS), has a well-established role in processing human biological motion (e.g., Grossman et al., 2000) as well as understanding the intentions that underlie others' movements or actions (e.g., Brass et al., 2007; for an overview of the functional properties of STS, see Lahnakoski et al., 2012; Deen et al., 2015). Recent evidence shows that PSTS is engaged by dynamic interacting human stimuli above-and-beyond non-interactive stimuli

Received Nov. 11, 2022; revised Feb. 20, 2023; accepted Mar. 12, 2023.

Author contributions: J.W., J.A., and K.K. designed research; J.W. and K.K. performed research; J.W. analyzed data; J.W. wrote the first draft of the paper; J.W., J.A., and K.K. edited the paper; J.W., J.A., and K.K. wrote the paper.

This work was supported by European Research Council under the European Union's Horizon 2020 research and innovation program (Grant Agreement 716974, "Becoming Social") to K.K. J.A. was supported by the European Research Council under the European Union's Horizon 2020 research and innovation program (Grant Agreement 802553, "ContentMAP").

Data are not available (consent to share data was not sought from child participants).

The authors declare no competing financial interests.

Correspondence should be addressed to Jon Walbrin at jon.walbrin@gmail.com.

<https://doi.org/10.1523/JNEUROSCI.2109-22.2023>

Copyright © 2023 the authors

(e.g., Centelles et al., 2011; Isik et al., 2017; Walbrin et al., 2018). Beyond visual analysis, MPFC responses are sometimes shown when probing mental state inferences while viewing interacting individuals (Iacoboni et al., 2004; Dolcos et al., 2012) but are absent when such inferences are not elicited (Isik et al., 2017; Walbrin et al., 2018). Thus, social interaction understanding potentially draws on diverse kinds of social information (that may, in part, be influenced by the cognitive processing goal(s) at hand, e.g., mentalizing, or not).

Currently, the few fMRI studies that have explored the developmental underpinnings of dyadic interaction processing broadly suggest gradual age-related changes. Sapey-Triomphe et al. (2017) showed age-related increases in fronto-parietal network regions, but common recruitment of PSTS across adults, adolescents, and children when discriminating interacting from non-interaction point-light dyads. Using similar stimuli, Walbrin et al. (2020) showed poorer differentiation of interaction versus non-interaction responses in a PSTS ROI for children relative to adults, and more graded differences when considering subgroups of children.

Indeed, gradual development is shown across social processes more generally. This is true for behavioral measures of interaction understanding (Hamlin et al., 2007; Balas et al., 2012; Centelles et al., 2013; Brey and Shutts, 2015; Goupil et al., 2022), and for mentalizing, body, face, and biological motion perception (Simion et al., 2008; Hadad et al., 2011; Weigelt et al., 2014; Wellman, 2014). This is also shown with fMRI measures, for example, via weaker or less specific activation responses in children (for mentalizing, biological motion, body, and face stimuli) (Carter and Pelphrey, 2006; Scherf et al., 2007; Lichtensteiger et al., 2008; Gweon et al., 2012; Ross et al., 2014; Deen et al., 2017) and via reduced functional segregation between social and non-social brain networks or connectivity strength differences within social brain networks (Richardson et al., 2018; Wang et al., 2018; O'Rawe et al., 2019; Morningstar et al., 2021).

In short, much remains to be learned about: (1) the development of social interaction understanding and (2) how constituent sources of social information meaningfully contribute to interaction understanding. Accordingly, we used a “supportive connectivity” analysis to test which seed areas of the social brain (i.e., areas that support body perception, social interaction recognition, and mentalizing) demonstrate connectivity that is related to interactive dyadic biological motion responses in STS. This follows previous work that demonstrates how local-level brain activity is strongly related to connectivity with distal brain areas that share similar computational goals (e.g., between face network areas) (Chen et al., 2017; Amaral et al., 2021; see also D. Lee et al., 2019; Walbrin and Almeida, 2021). Thus, beyond simple activation differences, this approach affords an insight into the sources of social information that support interactive biological motion processing in STS, and whether the influence of these sources changes across development.

Materials and Methods

Participants. Thirty-one children (aged between 6 and 12 years) and 29 adults took part in a previously published experiment (Walbrin et al., 2020). All subjects' data were reanalyzed for the current manuscript, except for 2 children and 1 adult who did not have connectivity data (i.e., did not complete the MRI task that connectivity was estimated from), resulting in final group sizes of 29 children (mean age = 9.10; SD = 1.86; 13 females) and 28 adults (mean age = 22.93; SD = 4.27; range = 18–35; 15 females). All subjects were neurotypical and right-handed. Children gave informed assent (consent was also given by a guardian of each child),

and they received gift vouchers (or toys of equivalent value) as compensation for participation. Adult subjects gave consent and received monetary compensation for participation. Ethical procedures were approved by the Bangor University psychology ethics board.

MRI tasks. Inside the scanner, two video tasks were completed: (1) A biological motion task that was used to estimate STS activation responses. This consisted of three runs of videos from three conditions (see Fig. 1b): interaction (INT; i.e., two profile-view human point-light figures interacting; for example, each figure gesturing toward the other), non-interaction (NON; i.e., two figures performing noninteractive actions separated by a vertical line; for example, one figure jumping, the other cycling), and scrambled interaction (SCR; i.e., average “motion-matched” versions of the INT stimuli where the coordinates of each point-light dot were randomly shifted to disrupt the perception of coherent biological motion; block length = 16 s, based on three videos of variable length that summed to 16 s; 3×16 s rest blocks, one presented at the beginning, middle, and end of each run; total run length = 144 s). Each run consisted of two blocks per condition, one presented in either half of each run, in counterbalanced order with the other conditions. In order to minimize head motion in children, no button response task was used. Instead, all participants were instructed to simply maintain attention throughout each run. Although behavioral performance measures were not obtained here, children (aged 4–10) show good discrimination of similar interactive and noninteractive biological motion stimuli (Centelles et al., 2013). (2) A “dynamic objects” task that was used here for the sole purpose of estimating “background” functional connectivity (i.e., regressing away the task design [stimulus-locked activation] from the fMRI time-series). Thus, task-related activation for the conditions of this localizer task was not analyzed here (for these results, see Walbrin et al., 2020). Participants completed three runs of this task that contained counterbalanced blocks of videos that depicted either moving faces, moving bodies, or moving objects (block length = 18 s [6×3 s videos]; four blocks per condition; 5×16 s rest blocks; total run length = 296 s). All three concatenated runs were used for connectivity estimation.

Head movement analysis. To minimize fatigue and head motion in children (e.g., Meissner et al., 2020), the scanning session was split into two halves (the biological motion task was always completed in the first half) with a short break where subjects came out of the scanner for ~5–10 min. For consistency, adults also took this break. Group differences in average head motion were analyzed by comparing head movement measures across subjects (e.g., Kang et al., 2003). Briefly explained, for each run (per subject), the mean absolute difference between head position at each TR and the average head position across the run was calculated. Two scores were created: one for translation movements (mean difference averaged across x , y , z), and another for rotation movements (mean difference averaged across roll, pitch, yaw). These values were then averaged across all runs, and entered into independent t tests. Children showed greater head movement than adults for both translation ($t_{(55)} = 5.19$, $p < 0.001$) and rotation measures ($t_{(55)} = 4.94$, $p < 0.001$). However, the overall amount of head motion was small (average translation in mm = children mean: 0.15, SD: 0.09; adults mean: 0.06, SD: 0.03; average rotation in degrees = children mean: 0.0028, SD: 0.0022; adults mean: 0.0008, SD: 0.0003). These differences are in line with similar trends that are routinely reported in developmental MRI work (for a detailed analysis and overview, see, e.g., Kang et al., 2003; see Meissner et al., 2020). Importantly, the main results reported in this manuscript provide strong evidence against the presence of problematic head motion in children (i.e., children show seed-specific effects that contradict the expectation of globally weaker effects arising from excessive head motion).

MRI parameters, preprocessing, and GLM estimation. Scanning was performed at Bangor University with a Philips 3T scanner. The same fMRI parameters were used for all data, as follows: T2*-weighted gradient-echo single-shot EPI pulse sequence (with SofTone noise reduction); TR = 2000 ms, TE = 30 ms, flip angle = 83°, FOV (mm) = 240 × 240 × 112, acquisition matrix = 80 × 78 (reconstruction matrix = 80); 32 contiguous axial slices in ascending order, acquired voxel size (mm) = 3 × 3 × 3.5 (reconstructed voxel size = 3 mm³). Four dummy

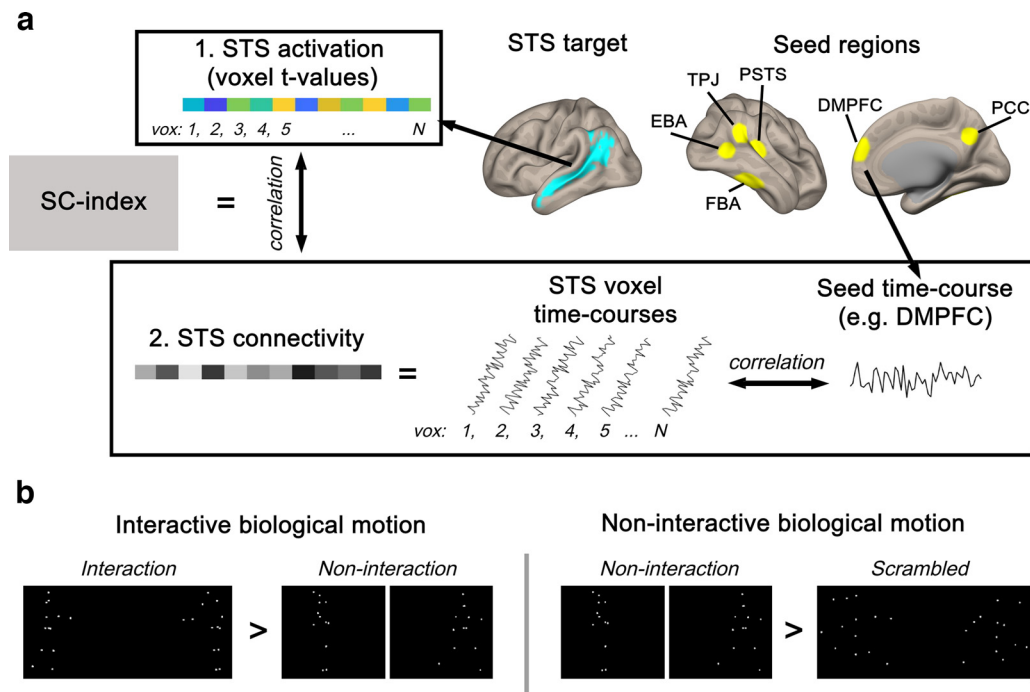


Figure 1. Overview of supportive connectivity estimation. **a**, The SC index is calculated as the Pearson's correlation between: (**a1**) STS activation [e.g., t values for interactive biological motion (interaction > non-interaction contrast)] and (**a2**) STS voxel-wise connectivity (Pearson's correlation coefficient) when seeding from a given seed region (e.g., DMPFC). **b**, Interactive and noninteractive biological motion contrasts are shown with representative video frames from example stimuli.

scans were discarded before image acquisition for each run. Structural images were obtained with the following parameters: T1-weighted image acquisition using a gradient echo, multishot turbo field echo pulse sequence, with a 5 echo average; TR = 12 ms, average TE = 3.4 ms, in 1.7 ms steps, total acquisition time = 136 s, FA = 8°, FOV = 240 × 240, acquisition matrix = 240 × 224 (reconstruction matrix = 240); 128 contiguous axial slices, acquired voxel size (mm) = 1.0 × 1.07 × 2.0 (reconstructed voxel size = 1 mm³).

Preprocessing and GLM estimation were performed with SPM12 (www.fil.ion.ucl.ac.uk/spm/software/spm12) for both tasks. All SPM12 default preprocessing parameters were used; but to ensure good alignment of data across the two halves of the session, the following steps were performed: (1) functional images were realigned for each sub-session separately; (2) T1 images, acquired in each sub-session, were then coregistered to their respective mean functional alignment image; and (3) the second sub-session data (T1 and functional images) were then coregistered to data from the first sub-session, bringing all data into alignment. Data were then normalized to MNI space (2 mm³ voxels) but were not smoothed, to better preserve voxel-level activation and connectivity estimates.

Block durations and onsets for each experimental condition (per run) were modeled by convolving the corresponding box-car time course with the SPM canonical HRF (without time or dispersion derivatives), with a high-pass filter of 128 s and autoregressive AR(1) model. Head motion parameters (three translation and three rotation axes) were modeled as nuisance regressors. Background connectivity (e.g., Fair et al., 2007; Cole et al., 2014; Walbrin and Almeida, 2021) was estimated from the dynamic objects task data, by regressing away task effects (i.e., convolving the canonical SPM12 HRF with the block-events for each condition) along with other confound regressors (i.e., white matter and CSF), and applying temporal bandpass filtering (0.01–0.1 Hz) using the CONN Toolbox (Whitfield-Gabrieli and Nieto-Castanon, 2012).

Target and seed region definition. Previously, we showed that activation to interactive biological motion is strongest in PSTS, but similar activation is also present in more anterior portions of the sulcus too (in both children and adults). Therefore, we measured activation across the entire STS region. STS target region masks were generated for each hemisphere, for each subject individually, using the Freesurfer “recon-

all” function (based on the Destrieux atlas parcellation). These masks span the entire length of the STS (see Fig. 1a; including horizontal and ascending posterior branches). Masks were normalized and resliced to the same image resolution as the functional data.

For seed region masks, coordinates were identified by inspecting MNI space meta-analysis brain maps generated for specific search terms from the Neurosynth database (www.neurosynth.org) (for a detailed overview of this method, see Yarkoni et al., 2011). Briefly explained, a whole-brain map is generated from the activation coordinates reported in previous fMRI studies that contain high-frequency usage of a given term (e.g., “social interaction”). Although this approach adopts a lenient criterion for publication inclusion (e.g., does not distinguish papers that contain neurotypical vs patient populations), each meta-analysis map was derived from >100 publications, and as such is large enough to capture average activation trends associated with each term (for validation of a similar approach, see Yarkoni et al., 2011). Moreover, we manually inspected the location of seed regions to ensure that they were consistent with those reported in prior work (e.g., coordinates reported in a mentalizing meta-analysis) (Schurz et al., 2014). We further note that the use of the same seed regions for both adults and children is justified, based on previous work showing strong spatial correspondence of category-specific responses between adults and infants (Deen et al., 2017) and similar work demonstrating the appropriateness of comparing localized fMRI responses between adults and children in common stereotactic space (Kang et al., 2003). Further, the main results reported here provide strong evidence against the problematic localization of seed regions in children (i.e., across both main analyses, children show evidence of stronger positive supportive connectivity effects than adults in each of the seed areas).

The locations of the six seed regions were identified (for each hemisphere) by selecting the voxel with the strongest magnitude for each seed area, that was associated with one of the following three search terms: (1) Body: EBA [MNI coordinates (x, y, z): right: 49, -72, 3; left: -46, -74, 4] and FBA [right: 44, -46, -20; left: -44, -46, -20]; (2) Mentalizing: temporo-parietal junction (TPJ) [right: 49, -58, 21; left: -50, -58, 21], dorsomedial PFC (DMPFC) [right: 7, 55, 22; left: -7, 55, 22], and PCC (posterior cingulate cortex) [right: 7, -57, 35; left: -7, -52, 38]. (3) Social interaction: PSTS [right: 48, -42, 8; left: -55, -52,

12]. Importantly, we note that, although we used the search term “social interaction” to identify the PSTS seed, we do not claim that this region is solely engaged by social interactions/interactive dyadic biological motion (e.g., PSTS is also responsive to single-human biological motion) (Allison et al., 2000; Grossman et al., 2000; Carter and Pelphrey, 2006) as well as the intentionality of others’ actions (e.g., Saxe et al., 2004; Pelphrey et al., 2004; Brass et al., 2007). The resulting seed regions (see Fig. 1a) consisted of 6-mm-radius spheres centered at peak coordinates (or slightly adjusted when the coordinate was close to the edge of the brain to avoid capturing nonbrain voxels within the sphere) and white matter voxels were removed (for each subject individually). Adjacent seed regions did not overlap. Importantly, because of the presence of seed regions within/bordering STS (i.e., PSTS and TPJ), we adopted a contralateral seeding approach for all seed regions. For example, for right STS target, we only used seed regions in the left hemisphere, and vice versa. This ensured that we never circularly extracted connectivity from voxels that overlapped both target and seed regions.

Supportive connectivity estimation. In each STS target region, we estimated the relationship between local activation and distal connectivity with the same approach as Chen et al. (2017) and Amaral et al. (2021), described as follows. First, we focused on STS activation to interactive biological motion, by extracting STS voxel t values for the INT > NON contrast (Fig. 1b). Specifically, this contrast was intended to capture interactive biological motion information (e.g., contingent movements/actions, person-directed movements) above-and-beyond (noninteractive) biological motion. In a follow-up analysis we examined STS activation to noninteractive biological motion, by extracting STS voxel t values for the NON > SCR contrast (Fig. 1b); this captures human biological information without the presence of interactive motion information.

A supportive connectivity index (SC index) was calculated for each seed region as follows (Fig. 1a). (1) For each measure of activation (e.g., interactive biological motion), we obtained an activation vector (t values) of all STS voxels (for each hemisphere separately). (2) For a given seed region, a connectivity vector was generated by correlating (Pearson’s r) the connectivity time course of each STS voxel with the mean time course of the seed region. (3) The activation and connectivity vectors were then correlated (Pearson’s r) to yield an SC index. Seed hemisphere was always contralateral to the STS target hemisphere. Subjects’ SC indices were Fisher-transformed before being entered into group-level tests.

Searchlight-seeding analysis. To test whether other brain areas, beyond the *a priori* seed regions featured in the main analyses, yield a significant SC index, we ran a whole-brain analysis, as follows. A searchlight consisting of ~100 contiguous voxels was iteratively centered on each gray matter voxel of the brain (white matter was masked out beforehand); the mean voxel time course was extracted and then correlated with voxel-wise time courses of STS to generate a connectivity vector that was then correlated with voxel-wise STS activation (as in the main analysis), and then the Fisher-transformed SC index was assigned to the central voxel of the corresponding searchlight. As such, the resulting maps show which brain areas “seed” a significant SC index. For each analysis, this was performed twice: once with the right and once with the left STS serving as target regions (target STS voxels were masked out from the searchlight space in the target hemisphere, but not in the other hemisphere).

Subject’s searchlight maps were smoothed (6 mm FWHM kernel) before group-level inference. To test which regions showed an SC index different from zero, in either group, one-sample t tests were run with threshold-free cluster enhancement based on 10,000 Monte Carlo simulations, for adults and children, and for each (target STS) hemisphere, separately. The resulting maps were thresholded at $Z > 1.65$ (no significantly negative effects were observed) and projected to a surface rendered brain (with the CONN toolbox) for visualization. To directly test for differences in SC index between age groups, independent t tests were performed (threshold-free cluster enhancement, 10,000 Monte Carlo simulations, maps thresholded at $Z > 1.65$ and $Z < -1.65$). Resulting inference maps for both adults and children were projected to the brain surface for visualization. For consistency with the contralateral target-seeding approach in the main analyses, contralateral searchlight coverage

is shown here on a single map (i.e., left hemisphere shows searchlight seeding to right STS, and right hemisphere shows seeding to left STS).

Experimental design and statistical analyses. For the main analysis, we considered the supportive connectivity of seed regions for interactive biological motion information. A three-way mixed ANOVA was used to assess statistical differences in SC index across three factors: (1) age group (adults, children); (2) seed region (PSTS, FBA, EBA, TPJ, DMPFC, PCC; repeated-measures factor); and (3) target region hemisphere (right STS, left STS; repeated-measures factor). A three-way ANOVA was also used for the follow-up analysis where we tested supportive connectivity for noninteractive biological motion. For conciseness, we only report significant ANOVA effects for interactions and follow-up t contrasts. In addition to direct comparisons of SC indices between groups, we also performed one-sample t tests against 0 (two-tailed) to test indirect group differences (e.g., one group may show >0 SC indices for a particular seed, but the other group might not). A Bonferroni-corrected threshold was calculated for each set of follow-up tests ($p = 0.008$ for both independent and one-sample tests). All reported tests survive correction unless explicitly stated. We further note the reporting of several uncorrected results here that we consider important to distinguish from marginal results (i.e., results with uncorrected p values closer to 0.01 than 0.05).

Results

Interactive biological motion: *a priori* seed analyses

We tested which of the six *a priori* seed regions share connectivity with STS that is, in turn, correlated with STS activation to interactive biological motion. A three-way mixed ANOVA (age group \times seed region \times target region hemisphere) revealed an interaction between age group and seed region ($F_{(5,275)} = 6.09$, $p = 0.001$, $\eta^2 = 0.100$; three-way interaction was not significant: $F_{(5,275)} = 0.11$, $p = 0.990$, $\eta^2 = 0.002$). Follow-up tests revealed two key results (Fig. 2a): First, adults showed a higher SC index than children in PSTS ($t_{(326,94)} = 2.88$, $p = 0.004$). A similar effect was shown for FBA but at an uncorrected level only ($t_{(326,94)} = 2.36$, $p = 0.019$). Similar trends for EBA were not significant ($t_{(326,94)} = 0.89$, $p = 0.373$). Second, for the remaining three seed regions, children showed trends toward higher SC indices than adults. This trend was significant in TPJ ($t_{(326,94)} = -2.85$, $p = 0.005$). Similar marginal trends for DMPFC and PCC were not significant (DMPFC: $t_{(326,94)} = -1.69$, $p = 0.092$; PCC: $t_{(326,94)} = -1.87$, $p = 0.062$). Additionally, an interaction between seed and target region hemisphere ($F_{(5,5)} = 3.00$, $p = 0.012$, $\eta^2 = 0.052$) indicated higher SC indices for left than right seed regions in PSTS ($t_{(329,89)} = 2.95$, $p = 0.003$) and EBA ($t_{(329,89)} = 2.76$, $p = 0.006$; other seed p values > 0.091). The age group \times target region hemisphere interaction was not significant ($F_{(1,55)} = 0.00$, $p = 0.993$, $\eta^2 = 0.000$).

In addition to the direct group comparisons above, we tested whether either group showed SC indices that are significantly different from zero for each of the six seed regions. One-sample t tests (two-tailed) were performed. As age group did not interact with hemisphere, we collapsed across hemispheres for each seed region. For adults, above-zero SC indices were shown for PSTS ($t_{(27)} = 4.03$, $p < 0.001$) and FBA ($t_{(27)} = 4.55$, $p < 0.001$), complementing the previous independent t test results for these regions. All other seed regions were not significant (p values > 0.286). For children, above-zero SC indices were shown for DMPFC ($t_{(28)} = 3.32$, $p < 0.001$) and TPJ at an uncorrected level ($t_{(28)} = 2.69$, $p = 0.012$). All other seeds were not significant (p values > 0.061). Together, these analyses suggest distinct roles of supportive connectivity of interactive biological motion for each age group: For adults, evidence is shown for PSTS and FBA, and in children for TPJ and DMPFC.

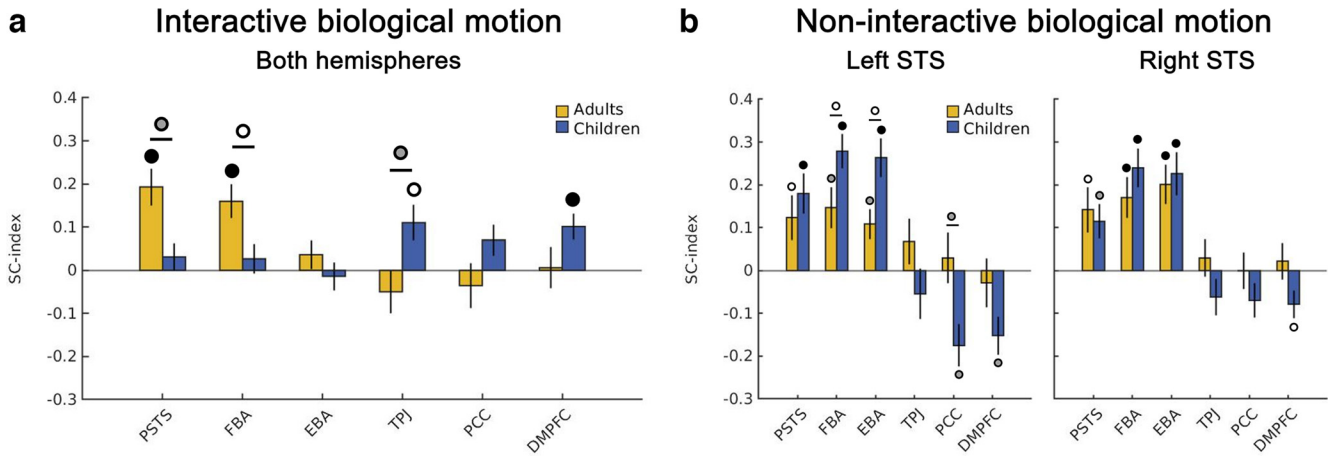


Figure 2. Bar charts represent group mean SC index from each seed region to STS (seeds are contralateral to STS hemisphere), for each age group, respectively, for: (a) interactive biological motion (plotted across both STS hemispheres combined; no age group × hemisphere interaction); and (b) noninteractive biological motion (plotted separately for each STS hemisphere following a significant age group × hemisphere interaction). Error bars indicate SEM. Filled black, filled gray, and unfilled circles represent *p* values of <0.001, <0.01, and <0.05, respectively.

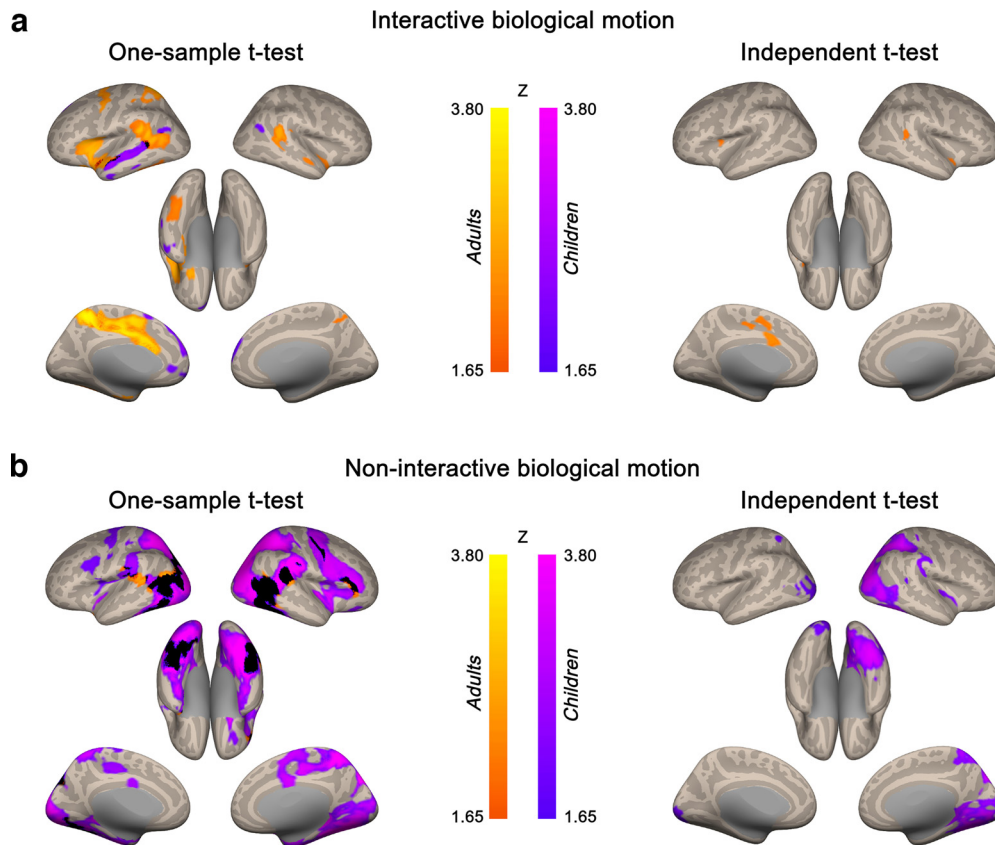


Figure 3. Surface maps represent group-level searchlight seeding analysis results. a, Results for interactive biological motion for one-sample *t* tests for each group (left) and independent *t* tests directly comparing the two groups (right). b, Results for noninteractive biological motion for one-sample *t* tests (left) and independent *t* tests (right). Orange scale represents significant coverage for adults (coverage significantly different from zero for one-sample *t* tests, or significantly greater than children for independent *t* tests). Purple scale represents significant coverage for children. Black coverage represents overlap between groups for the one-sample *t* tests.

Interactive biological motion: exploratory searchlight seeding analyses

Next, we ran searchlight analyses to test whether brain areas beyond the *a priori* seed areas showed a significant SC index. One-sample *t* test maps are shown in Figure 3a (left); these maps show which areas yield a significantly “above-zero” SC index, for each age group separately (no significant negative effects were observed for either group). Two main observations are noted

here. First, the two groups showed distinct searchlight coverage, with very minimal overlap. Most notably, bilateral PSTS was shown for adults, while children showed unique coverage more posteriorly, in bilateral posterior temporo-occipital cortex, along with extensive coverage along the middle-to-anterior STS (left hemisphere). Second, coverage is more diffuse for adults, predominantly left hemisphere effects in middle fusiform gyrus, middle cingulate cortex, dorsal precentral gyrus, superior parietal

cortex, and anterior STS/superior temporal gyrus (small right hemisphere clusters were shown for anterior STS, insula, and posterior cingulate). Children also showed unique coverage in MPFC (dorsal and ventral aspects) that was mostly confined to the left hemisphere. Direct comparisons between groups (independent t test; Fig. 3*a*, right), show small clusters in right PSTS and anterior superior temporal gyrus/insula, along with left insula and middle cingulate cortex, indicating a significantly higher SC index for adults than children in these areas. Together, these results show an age-related difference in terms of how activation to interactive biological motion in STS is related to functional connectivity to the wider brain.

Follow-up analyses: noninteractive biological motion

We next tested SC indices for seed regions when considering STS activation to noninteractive biological motion. The primary aim of these analyses was to test whether the results in the preceding analyses are specific to interactive biological motion. A three-way mixed ANOVA (age group \times seed region \times target region hemisphere) revealed a significant three-way interaction ($F_{(5,275)} = 2.44$, $p = 0.035$, $\eta^2 = 0.042$). We focused on follow-up comparisons between the two age groups (i.e., comparing SC index between adults and children, per each seed region, per hemisphere; see Fig. 2*b*). Unlike for interactive biological motion, few differences were shown when directly comparing the two groups, and these results were specific to right hemisphere seed regions. Children showed a significantly lower (more negative) SC index than adults for PCC ($t_{(500.77)} = 3.08$, $p = 0.002$). Children showed an uncorrected trend toward a higher SC index than adults in EBA ($t_{(500.77)} = -2.33$, $p = 0.020$) and a marginal trend in FBA ($t_{(500.77)} = -1.98$, $p = 0.048$). No differences were shown for the remaining right hemisphere, or any left hemisphere, seed regions (right hemisphere seed p values > 0.171 ; left hemisphere seed p values > 0.064).

Next, one-sample t tests (two-tailed) were conducted. Adults showed above-zero indices in FBA (right: $t_{(27)} = 3.07$, $p = 0.005$; left: $t_{(27)} = 3.55$, $p = 0.001$) and EBA (right: $t_{(27)} = 3.12$, $p = 0.004$; left: $t_{(27)} = 4.39$, $p = 0.002$). Similar trends were shown at an uncorrected level only in PSTS (right: $t_{(27)} = 2.35$, $p = 0.026$; left: $t_{(27)} = 2.69$, $p = 0.012$). Adults did not show differences in any other area (all other seed p values > 0.506). For children, above-zero SC indices were shown for FBA (right: $t_{(28)} = 6.94$, $p < 0.001$; left: $t_{(28)} = 5.25$, $p < 0.001$), EBA (right: $t_{(28)} = 5.84$, $p < 0.001$; left: $t_{(28)} = 4.46$, $p < 0.001$), and PSTS (right: $t_{(28)} = 3.79$, $p < 0.001$; left: $t_{(28)} = 2.84$, $p = 0.008$). Children also showed significantly negative SC indices for bilateral DMPFC (right: $t_{(28)} = -3.41$, $p = 0.002$; left: $t_{(28)} = -2.42$, $p = 0.022$), and right PCC ($t_{(28)} = -3.53$, $p = 0.002$). All other seeds were not significant (all other seed p values > 0.160). Importantly, these analyses show that the group differences demonstrated for interactive biological motion are not shown for noninteractive biological motion.

Finally, complementary searchlight analyses were conducted. Two main observations are noted from the one-sample t test maps (Fig. 3*b*, left; no significant, negative SC index coverage was observed). First, overlap is shown in bilateral lateral occipitotemporal cortex and fusiform gyrus (consistent with EBA and FBA regions), along with right lateralized supramarginal gyrus, precentral gyrus, and inferior frontal gyrus. Second, adults showed unique coverage in left superior temporal gyrus only, while children showed extensive unique coverage across many brain areas, including PSTS, dorsal precentral gyrus, superior

parietal cortex, ventral temporal cortex, lateral occipital cortex, middle cingulate cortex, and lateral PFC. When directly comparing between groups (i.e., independent t test map; Fig. 3*b*, right), children showed a stronger SC index than adults in many areas (and adults did not show significantly higher SC index in any area); this coverage was stronger in right hemisphere regions (i.e., posterior and inferior parietal cortex; posterior cingulate cortex; lateral, ventral, and medial posterior temporal cortex), with effects also in left superior parietal cortex and occipitotemporal cortex). These results suggest that noninteractive biological motion processing in STS is supported by connectivity to EBA, FBA, and PSTS in adults. In children, similar coverage is shown for EBA, FBA, and PSTS, but also much broader coverage in the wider brain, indicating that immature biological motion responses are, in part, characterized by widespread connectivity to the rest of the brain.

Discussion

Here, we show that different connectivity supports social interaction processing in adults and children. Specifically, supportive connectivity to contralateral PSTS (which favors biological motion) (e.g., Grossman et al., 2000; Gobbin and Haxby, 2007), action-intention understanding (e.g., Saxe et al., 2004; Brass et al., 2007), and dynamic interactive information (e.g., Isik et al., 2017; Walbrin et al., 2018) and body-prefering FBA, is shown in adults. By contrast, connectivity to DMPFC and TPJ, two areas that form central nodes of the mentalizing network (e.g., Schurz et al., 2014; Richardson et al., 2018), is shown in children. Importantly, these connectivity differences are specific to interactive biological motion.

We suggest that these age differences in supportive connectivity reveal different cognitive strategies that support understanding interactive biological motion, that is, that children may engage in more effortful, covert inferential processing than adults, who rely on more overt inferences (i.e., children tend more toward making hidden mental state inferences, while adults understand the immediate intentions of interactions via observable actions). Indeed, previous meta-analysis results (Schurz et al., 2014) show that TPJ and MPFC are core mentalizing network areas that are routinely engaged by tasks that probe covert inferences (e.g., correctly inferring the beliefs of a character in a story, correctly associating a personality trait with the behavior of an individual, and inferring the strategy of another player in a game, e.g., rock, paper, scissors). Similarly, previous studies that use visual interaction stimuli and prompt participants to make covert inferential judgments show MPFC activation (Iacoboni et al., 2004; Dolcos et al., 2012), while such activation is typically missing from studies that do not prompt these kinds of judgments (Georgescu et al., 2014; Isik et al., 2017; Walbrin et al., 2018, 2020).

Previous work shows that, relative to adults, children and adolescents demonstrate increased MPFC activation (Blakemore et al., 2007; Kobayashi et al., 2007; Pfeifer et al., 2007; Sebastian et al., 2012) and connectivity between MPFC and other social brain areas while performing tasks that probe covert judgments about other people (Burnett and Blakemore, 2009; Somerville et al., 2013). The role of MPFC in these studies has been interpreted as reflecting an increase in cognitive effort required for making mental state inferences (Blakemore, 2012), as well as a general functional mechanism in service of higher-level skill acquisition (e.g., increased recruitment of MPFC while learning to master complex cognitive abilities) (Johnson, 2011). In the context of the

current findings, increased reliance on covert inferential processing may be a necessary mechanism that supports a gradual shift toward a more automatic (and less cognitively effortful) form of interaction understanding in adults.

Accordingly, mature interaction responses are supported by connectivity to (contralateral) PSTS (as well as FBA). While PSTS has long been associated with human biological motion perception (Allison et al., 2000; Grossman et al., 2000; Carter and Pelphrey, 2006; Gobbini and Haxby, 2007), it is also associated - and potentially partially confounded with processing the immediate, overt intentions that underlie others' movements and actions (Pelphrey et al., 2004; Saxe et al., 2004; Brass et al., 2007; Vander Wyk et al., 2009; Deen and Saxe, 2012; Gao et al., 2012; S. M. Lee et al., 2014). For example, Saxe et al. (2004) demonstrate PSTS involvement when subjects viewed stimuli depicting a walking human figure momentarily pausing behind a bookshelf (vs no momentary pausing); the immediate intention (i.e., the person is browsing) is grasped with relatively minimal abstraction compared with higher-level covert judgments (e.g., the person likes to read, they are curious) that are supported by areas of the mentalizing network. It is perhaps inevitable then that PSTS is strongly engaged by dynamic social interactions, which involve perceiving and processing both action and intention information, in adults (Centelles et al., 2011; Georgescu et al., 2014; Isik et al., 2017; Walbrin et al., 2018, 2020; Wordecha et al., 2018; Walbrin and Koldewyn, 2019; Bellot et al., 2021; Masson and Isik, 2021; Landsiedel et al., 2022).

In short, adults may rely on the PSTS to grasp the immediate, overt intentional contents of interactions, a complex ability that likely undergoes refinement across development. By contrast, in lieu of this ability, children may rely more on an effortful, covert strategy that depends on areas of the mentalizing network. Although the present data cannot reveal the exact nature of the kinds of inferences that children make, we consider two possibilities. First, children may build a hierarchical "piece-by-piece" understanding of interactions that requires multiple inferences (e.g., "the two people are moving quickly" > "they seem angry" > "they are arguing"). Second, children may engage more in cognitive and affective mental state attributions (e.g., "they are angry at each other," "they don't like each other"). By contrast, adults may understand the gist of an interaction without covert mental state inferences (e.g., the kinematics of the two people imply an argument; as experience suggests that anger is typical for most arguments, inferring that the interactors are angry is redundant, and not necessary for a basic understanding of the scenario). However, these possibilities are not exhaustive, and future studies may better specify the kinds of spontaneous attributions that children make in these scenarios.

We also consider that neural maturation is an important factor when considering the current results. For example, gray matter volume changes occur relatively slowly in STS compared with most other brain areas (Gogtay et al., 2004). Other similar morphologic changes of STS, such as reduction in cortical thickness (Mills et al., 2014) and changes in sulcal depth (Bonte et al., 2014), have also been shown. These structural changes across development undoubtedly contribute to the present age-related effects (e.g., by refining the functional organization of STS).

We also note both differences and commonalities across groups in the involvement of body-perception areas. FBA demonstrates supportive connectivity of interactive biological motion in adults but not children. This aligns with previous findings that FBA (as well as EBA) shows sensitivity to dyadic body cues, such

as facing direction (Abassi and Papeo, 2020), and apparent congruency of interactants (Quadflieg et al., 2015) that are likely important computations for differentiating interactive from noninteractive biological motion. Both children and adults also showed FBA involvement for noninteractive biological motion, suggesting that the computations in this area are also relevant for biological motion per se (i.e., differentiating non-interactive biological motion from scrambled motion).

By comparison, supportive connectivity effects for EBA were not shown (for either age group) for interactive biological motion, but instead these effects were shown for noninteractive biological motion, suggesting a more general involvement of this area in supporting body and biological motion processing per se. This lack of involvement, at first glance, appears at odds with previous work that links EBA with the processing of dyadic stimuli (Quadflieg et al., 2015; Walbrin and Koldewyn, 2019; Abassi and Papeo, 2020; Landsiedel et al., 2022). This discrepancy might in part relate to stimulus differences: the stimuli used across these studies contained strong body-form information that is known to drive EBA responses (e.g., Downing et al., 2006) but is comparatively weaker (though still present in point-light stimuli) (e.g., Vangeneugden et al., 2014), and therefore may not contribute sufficiently to STS responses that differentiate interactive and non-interactive biological motion in these data. Interestingly, a recent study showed that the degree of feedforward connectivity from EBA to PSTS is dependent on the kind of movement portrayed by point-light dyads (i.e., moving toward vs moving away) (Bellot et al., 2021). However, methodological differences in the present study make a direct comparison difficult (i.e., directed dynamic causal modeling with mean ROI time courses vs bidirectional background connectivity with voxel-wise STS time courses). Parsimoniously, we suggest that, given different response preferences between ventral body areas, that is, stronger preference for body part and whole-body stimuli in EBA and FBA, respectively (Taylor et al., 2007), stronger supportive connectivity of FBA than EBA likely reflects the higher relevance of elaborated whole-body information that is more useful for whole-body interactive biological motion discrimination.

Finally, we note several limitations and aspects of the current experiment that merit further research. First, we are agnostic as to the causal nature of the present connectivity effects. Future research may use brain stimulation approaches to directly target and perturb the contribution of individual seed areas. Second, we used sparse, visually controlled point-light stimuli that do not contain information that would otherwise be important in most interactive contexts (e.g., spoken language), and as such, future research may focus on other interactive information not present in the current stimuli. Third, we demonstrate compelling effects when considering a broad age range of children, but future work is needed to provide a more fine-grained developmental understanding across childhood, as well as to explore continued change across adolescence.

In conclusion, we show age-related differences in how the functional connectivity of social brain areas supports interactive biological motion processing in STS. These results are an important first step toward understanding how distinct sources of social information may contribute to social interaction understanding in the brain across development.

References

- Abassi E, Papeo L (2020) The representation of two-body shapes in the human visual cortex. *J Neurosci* 40:852–863.
- Allison T, Puce A, McCarthy G (2000) Social perception from visual cues: role of the STS region. *Trends Cogn Sci* 4:267–278.

- Amaral L, Bergström F, Almeida J (2021) Overlapping but distinct: distal connectivity dissociates hand and tool processing networks. *Cortex* 140:1–13.
- Balas B, Kanwisher N, Saxe R (2012) Thin-slice perception develops slowly. *J Exp Child Psychol* 112:257–264.
- Bellot E, Abassi E, Papeo L (2021) Moving toward versus away from another: how body motion direction changes the representation of bodies and actions in the visual cortex. *Cereb Cortex* 31:2670–2685.
- Bonte M, Hausfeld L, Scharke W, Valente G, Formisano E (2014) Task-dependent decoding of speaker and vowel identity from auditory cortical response patterns. *J Neurosci* 34:4548–4557.
- Blakemore SJ (2012) Imaging brain development: the adolescent brain. *Neuroimage* 61:397–406.
- Blakemore SJ, den Ouden H, Choudhury S, Frith C (2007) Adolescent development of the neural circuitry for thinking about intentions. *Soc Cogn Affect Neurosci* 2:130–139.
- Brass M, Schmitt RM, Spengler S, Gergely G (2007) Investigating action understanding: inferential processes versus action simulation. *Curr Biol* 17:2117–2121.
- Brey E, Shutts K (2015) Children use nonverbal cues to make inferences about social power. *Child Dev* 86:276–286.
- Burnett S, Blakemore SJ (2009) Functional connectivity during a social emotion task in adolescents and in adults. *Eur J Neurosci* 29:1294–1301.
- Carter EJ, Pelphrey KA (2006) School-aged children exhibit domain-specific responses to biological motion. *Soc Neurosci* 1:396–411.
- Centelles L, Assaiante C, Nazarian B, Anton JL, Schmitz C (2011) Recruitment of both the mirror and the mentalizing networks when observing social interactions depicted by point-lights: a neuroimaging study. *PLoS One* 6:e15749.
- Centelles L, Assaiante C, Etchegoyhen K, Bouvard M, Schmitz C (2013) From action to interaction: exploring the contribution of body motion cues to social understanding in typical development and in autism spectrum disorders. *J Autism Dev Disord* 43:1140–1150.
- Chen Q, Garcea FE, Almeida J, Mahon BZ (2017) Connectivity-based constraints on category-specificity in the ventral object processing pathway. *Neuropsychologia* 105:184–196.
- Cole MW, Bassett DS, Power JD, Braver TS, Petersen SE (2014) Intrinsic and task-evoked network architectures of the human brain. *Neuron* 83:238–251.
- Deen B, Koldewyn K, Kanwisher N, Saxe R (2015) Functional organization of social perception and cognition in the superior temporal sulcus. *Cereb Cortex* 25:4596–4609.
- Deen B, Richardson H, Dilks DD, Takahashi A, Keil B, Wald LL, Kanwisher N, Saxe R (2017) Organization of high-level visual cortex in human infants. *Nat Commun* 8:1–10.
- Deen B, Saxe R (2012) Neural correlates of social perception: the posterior superior temporal sulcus is modulated by action rationality, but not animacy. *Proceedings of the Annual Meeting of the Cognitive Science Society*. Sapporo, Japan.
- Dolcos S, Sung K, Argo JJ, Flor-Henry S, Dolcos F (2012) The power of a handshake: neural correlates of evaluative judgments in observed social interactions. *J Cogn Neurosci* 24:2292–2305.
- Downing PE, Chan AY, Peelen MV, Dodds CM, Kanwisher N (2006) Domain specificity in visual cortex. *Cereb Cortex* 16:1453–1461.
- Fair DA, Schlaggar BL, Cohen AL, Miezin FM, Dosenbach NU, Wenger KK, Fox MD, Snyder AZ, Raichle ME, Petersen SE (2007) A method for using blocked and event-related fMRI data to study 'resting state' functional connectivity. *Neuroimage* 35:396–405.
- Gao T, Scholl BJ, McCarthy G (2012) Dissociating the detection of intentionality from animacy in the right posterior superior temporal sulcus. *J Neurosci* 32:14276–14280.
- Georgescu AL, Kuzmanovic B, Santos NS, Tepes R, Bente G, Tittgemeyer M, Vogeley K (2014) Perceiving nonverbal behavior: neural correlates of processing movement fluency and contingency in dyadic interactions. *Hum Brain Mapp* 35:1362–1378.
- Gobbini MI, Haxby JV (2007) Neural systems for recognition of familiar faces. *Neuropsychologia* 45:32–41.
- Gogtay N, Giedd JN, Lusk L, Hayashi KM, Greenstein D, Vaituzis AC, Nugent TF, Herman DH, Clasen LS, Toga AW, Rapoport JL, Thompson PM (2004) Dynamic mapping of human cortical development during childhood through early adulthood. *Proc Natl Acad Sci USA* 101:8174–8179.
- Goupil N, Papeo L, Hochmann JR (2022) Visual perception grounding of social cognition in preverbal infants. *Infancy* 27:210–231.
- Grossman E, Donnelly M, Price R, Pickens D, Morgan V, Neighbor G, Blake R (2000) Brain areas involved in perception of biological motion. *J Cogn Neurosci* 12:711–720.
- Gweon H, Dodell-Feder D, Bedny M, Saxe R (2012) Theory of mind performance in children correlates with functional specialization of a brain region for thinking about thoughts. *Child Dev* 83:1853–1868.
- Hadad BS, Maurer D, Lewis TL (2011) Long trajectory for the development of sensitivity to global and biological motion. *Dev Sci* 14:1330–1339.
- Hamlin JK, Wynn K, Bloom P (2007) Social evaluation by preverbal infants. *Nature* 450:557–559.
- Iacoboni M, Lieberman MD, Knowlton BJ, Molnar-Szakacs I, Moritz M, Throop CJ, Fiske AP (2004) Watching social interactions produces dorsomedial prefrontal and medial parietal BOLD fMRI signal increases compared to a resting baseline. *Neuroimage* 21:1167–1173.
- Isik L, Koldewyn K, Beeler D, Kanwisher N (2017) Perceiving social interactions in the posterior superior temporal sulcus. *Proc Natl Acad Sci USA* 114:E9145–E9152.
- Johnson MH (2011) Interactive specialization: a domain-general framework for human functional brain development? *Dev Cogn Neurosci* 1:7–21.
- Kang HC, Burgund ED, Lugar HM, Petersen SE, Schlaggar BL (2003) Comparison of functional activation foci in children and adults using a common stereotaxic space. *Neuroimage* 19:16–28.
- Kobayashi C, Glover GH, Temple E (2007) Children's and adults' neural bases of verbal and nonverbal 'theory of mind.' *Neuropsychologia* 45:1522–1532.
- Lahnakoski JM, Glerean E, Salmi J, Jääskeläinen IP, Sams M, Hari R, Nummenmaa L (2012) Naturalistic fMRI mapping reveals superior temporal sulcus as the hub for the distributed brain network for social perception. *Front Hum Neurosci* 6:233.
- Landsiedel J, Daughters K, Downing PE, Koldewyn K (2022) The role of motion in the neural representation of social interactions in the posterior temporal cortex. *Neuroimage* 262:119533.
- Lee D, Mahon BZ, Almeida J (2019) Action at a distance on object-related ventral temporal representations. *Cortex* 117:157–167.
- Lee SM, Gao T, McCarthy G (2014) Attributing intentions to random motion engages the posterior superior temporal sulcus. *Soc Cogn Affect Neurosci* 9:81–87.
- Lichtensteiger J, Loenneker T, Bucher K, Martin E, Klaver P (2008) Role of dorsal and ventral stream development in biological motion perception. *Neuroreport* 19:1763–1767.
- Masson HL, Isik L (2021) Functional selectivity for social interaction perception in the human superior temporal sulcus during natural viewing. *Neuroimage* 245:118741.
- Meissner TW, Walbrin J, Nordt M, Koldewyn K, Weigelt S (2020) Head motion during fMRI tasks is reduced in children and adults if participants take breaks. *Dev Cogn Neurosci* 44:100803.
- Mills KL, Lalonde F, Clasen LS, Giedd JN, Blakemore SJ (2014) Developmental changes in the structure of the social brain in late childhood and adolescence. *Soc Cogn Affect Neurosci* 9:123–131.
- Morningstar M, French RC, Mattson WI, Englot DJ, Nelson EE (2021) Social brain networks: resting-state and task-based connectivity in youth with and without epilepsy. *Neuropsychologia* 157:107882.
- O'Rawe JF, Huang AS, Klein DN, Leung HC (2019) Posterior parietal influences on visual network specialization during development: an fMRI study of functional connectivity in children ages 9 to 12. *Neuropsychologia* 127:158–170.
- Pelphrey KA, Morris JP, McCarthy G (2004) Grasping the intentions of others: the perceived intentionality of an action influences activity in the superior temporal sulcus during social perception. *J Cogn Neurosci* 16:1706–1716.
- Pfeifer JH, Lieberman MD, Dapretto M (2007) 'I know you are but what am I?!' Neural bases of self-and social knowledge retrieval in children and adults. *J Cogn Neurosci* 19:1323–1337.
- Quadflieg S, Koldewyn K (2017) The neuroscience of people watching: how the human brain makes sense of other people's encounters. *Ann NY Acad Sci* 1396:166–182.
- Quadflieg S, Gentile F, Rossion B (2015) The neural basis of perceiving person interactions. *Cortex* 70:5–20.

- Richardson H, Lisandrelli G, Riobueno-Naylor A, Saxe R (2018) Development of the social brain from age three to twelve years. *Nat Commun* 9:1–12.
- Ross PD, de Gelder B, Crabbe F, Grosbras MH (2014) Body-selective areas in the visual cortex are less active in children than in adults. *Front Hum Neurosci* 8:941.
- Sapey-Triomphe LA, Centelles L, Roth M, Fonlupt P, Henaff MA, Schmitz C, Assaiante C (2017) Deciphering human motion to discriminate social interactions: a developmental neuroimaging study. *Soc Cogn Affect Neurosci* 12:340–351.
- Saxe R, Xiao DK, Kovacs G, Perrett DI, Kanwisher N (2004) A region of right posterior superior temporal sulcus responds to observed intentional actions. *Neuropsychologia* 42:1435–1446.
- Scherf KS, Behrmann M, Humphreys K, Luna B (2007) Visual category-selectivity for faces, places and objects emerges along different developmental trajectories. *Dev Sci* 10:F15–F30.
- Schurz M, Radua J, Aichhorn M, Richlan F, Perner J (2014) Fractionating theory of mind: a meta-analysis of functional brain imaging studies. *Neurosci Biobehav Rev* 42:9–34.
- Sebastian CL, Fontaine NM, Bird G, Blakemore SJ, De Brito SA, McCrory EJ, Viding E (2012) Neural processing associated with cognitive and affective Theory of Mind in adolescents and adults. *Soc Cogn Affect Neurosci* 7:53–63.
- Simion F, Regolin L, Bulf H (2008) A predisposition for biological motion in the newborn baby. *Proc Natl Acad Sci USA* 105:809–813.
- Somerville LH, Jones RM, Ruberry EJ, Dyke JP, Glover G, Casey BJ (2013) The medial prefrontal cortex and the emergence of self-conscious emotion in adolescence. *Psychol Sci* 24:1554–1562.
- Taylor JC, Wiggett AJ, Downing PE (2007) Functional MRI analysis of body and body part representations in the extrastriate and fusiform body areas. *J Neurophysiol* 98:1626–1633.
- Vander Wyk BC, Hudac CM, Carter EJ, Sobel DM, Pelphrey KA (2009) Action understanding in the superior temporal sulcus region. *Psychol Sci* 20:771–777.
- Vangeneugden J, Peelen MV, Tadin D, Battelli L (2014) Distinct neural mechanisms for body form and body motion discriminations. *J Neurosci* 34:574–585.
- Walbrin J, Almeida J (2021) High-level representations in human occipito-temporal cortex are indexed by distal connectivity. *J Neurosci* 41:4678–4685.
- Walbrin J, Koldewyn K (2019) Dyadic interaction processing in the posterior temporal cortex. *Neuroimage* 198:296–302.
- Walbrin J, Downing P, Koldewyn K (2018) Neural responses to visually observed social interactions. *Neuropsychologia* 112:31–39.
- Walbrin J, Mihai I, Landsiedel J, Koldewyn K (2020) Developmental changes in visual responses to social interactions. *Dev Cogn Neurosci* 42:100774.
- Wang X, Zhu Q, Song Y, Liu J (2018) Developmental reorganization of the core and extended face networks revealed by global functional connectivity. *Cereb Cortex* 28:3521–3530.
- Weigelt S, Koldewyn K, Dilks DD, Balas B, McKone E, Kanwisher N (2014) Domain-specific development of face memory but not face perception. *Dev Sci* 17:47–58.
- Wellman HM (2014) *Making minds: how theory of mind develops*. Oxford: Oxford UP.
- Whitfield-Gabrieli S, Nieto-Castanon A (2012) Conn: a functional connectivity toolbox for correlated and anticorrelated brain networks. *Brain Connect* 2:125–141.
- Wordecha M, Jarkiewicz M, Kossowski B, Lee J, Marchewka A (2018) Brain correlates of recognition of communicative interactions from biological motion in schizophrenia. *Psychol Med* 48:1862–1871.
- Yarkoni T, Poldrack RA, Nichols TE, Van Essen DC, Wager TD (2011) Large-scale automated synthesis of human functional neuroimaging data. *Nat Methods* 8:665–670.